Surface Pattern Recognition by a Colloidal Particle

Efrosini Kokkoli† and Charles F. Zukoski*

Department of Chemical Engineering, Beckman Institute for Advanced Science and Technology, University of Illinois at Urbana-Champaign, Urbana, Illinois 61801

Received April 24, 2000. In Final Form: November 2, 2000

This paper's focus is on understanding how surface heterogeneity alters surface forces. An atomic force microscope was used to measure interactions between a 20 μm hydrophobic ($-CH_3$) sphere and a patterned self-assembled monolayer surface of alkanethiols that consists of hydrophobic ($-CH_3$) and hydrophilic ($-COOH$) stripes of controlled width from 0.27 to 2.9 μm. Of significance to this study is the ratio of the particle radius to the stripe size. This ratio varied from 3.5 to 37, as a heterogeneous patterning on a length scale much larger than the sphere cannot affect the force. The results demonstrate that hydrophobic and hydrophilic interactions are not additive and the net interaction between these kind of surfaces depends on the relative size of hydrophobic and hydrophilic sites on the surface. Independent of whether the hydrophobic sphere is positioned on top of a hydrophobic or hydrophilic area, we measure repulsions, with the same strength and decay length of the electrostatic interaction. The magnitude of the heterogeneous energy is greatest when the patch size is smallest. Our results indicate that interactions, jump into contact distances and adhesion data, between a 20 μm methyl terminated sphere and a heterogeneous surface that has equal methyl and carboxylic acid areas will average. In all other cases, when the surface has unequal amounts of hydrophobic and hydrophilic areas, the hydrophobic sphere will clearly differentiate between the different patches and will accurately map high and low adhesion areas on the surface.

Introduction

Hydrophobic and hydrophilic interactions are two major intermolecular forces between nonpolar and polar sites of macromolecules or materials surfaces in solution. Previous studies have focused on the interactions between homogeneous hydrophobic[1−12] or hydrophilic[13−18] surfaces. However, in the majority of industrial and technological areas surfaces are heterogeneous with hydrophobic and hydrophilic sites, at both the microscopic and macroscopic level. Intermolecular interactions in a heterogeneous system will be a combination of van der Waals, electrostatic, hydrophobic, and hydrophilic forces. Due to the complexity of the phenomenon, interactions between heterogeneous surfaces have received much less attention. Since hydrophilic groups affect the structure of the water around them, this would compete with the very different structure that water molecules would adopt near a hydrophobic surface. This observation suggests that the hydrophobic interaction is nonadditive and that the net interaction can be extremely complex.

The degree of surface heterogeneity (i.e., hydrophilic−hydrophobic balance and charge distribution) is essential to the properties of biomolecules, colloidal particles, and surfaces of industrial interest. Previous studies demonstrate that the surface characteristics, such as the Debye length, magnitude and range of the forces, and ease of fusion, of a two-phase heterogeneous lipid bilayer surface vary between regions.[19] Structural studies have shown that nonpolar amino acids constitute about half of the surface area of proteins and they are organized as hydrophobic surface clusters.[20,21] This hydrophobic character of a protein may determine its solubility in aqueous media. The surface charge also appears to play an important role in protein properties such as deactivation and the binding of substrates to enzymes.[22] Understanding of the influence of patch size on interactions is in a poor state of development.

Particle attachment is mediated by surface forces, and the spatial distribution of these forces plays a central role in the recognition and attachment of particles to heterogeneous surfaces. When surfaces consist of hydrophobic and hydrophilic patches, descriptions of the net force experienced by an approaching particle and this particle's ability to distinguish the location of the different patches is of paramount importance in biological specificity and patterned materials formation.[23−25]

† Present address: 159 Goessmann Laboratory, Department of Chemical Engineering, University of Massachusetts at Amherst, Amherst, MA 01003.

(1) Israelachvili, J.; Pashley, R. M. *Nature* **1982**, *300*, 341.
(2) Israelachvili, J.; Pashley, R. M. *J. Colloid Interface Sci.* **1984**, *98*, 500.
(3) Pashley, R. M.; McGuiggan, P. M.; Ninham, B. W.; Evans, D. F. *Science* **1985**, *229*, 1088.
(4) Claesson, P. M.; Christenson, H. K. *J. Phys. Chem.* **1988**, *92*, 1650.
(5) Christenson, H. K.; Claesson, P. M. *Science* **1988**, *239*, 390.
(6) Rabinovich, Ya. I.; Derjaguin, B. V. *Colloids Surf.* **1988**, *30*, 243.
(7) Christenson, H. K.; Claesson, P. M.; Berg, J.; Herder, P. C. *J. Phys. Chem.* **1989**, *93*, 1472.
(8) Christenson, H. K.; Fang, J.; Ninham, B. W.; Parker, J. L. *J. Phys. Chem.* **1990**, *94*, 8004.
(9) Tsao, Y.-H.; Yang, S. X.; Evans, D. F.; Wennerström, H. *Langmuir* **1991**, *7*, 3154.
(10) Christenson, H. K.; Claesson, P. M.; Parker, J. L. *J. Phys. Chem.* **1992**, *96*, 6725.
(11) Tsao, Y.-H.; Evans, D. F.; Wennerström, H. *Science* **1993**, *262*, 547.
(12) Rabinovich, Ya. I.; Yoon, R.-H. *Langmuir* **1994**, *10*, 1903.
(13) Meagher, L. *J. Colloid Interface Sci.* **1992**, *152*, 293.
(14) Ducker, W. A.; Senden, T. J.; Pashley, R. M. *Langmuir* **1992**, *8*, 1831.
(15) Biggs, S.; Mulvaney, P. *J. Chem. Phys.* **1994**, *100*, 8501
(16) Chapel, J.-P. *Langmuir* **1994**, *10*, 4237.
(17) Vigil, G.; Xu, Z.; Steinberg, S.; Israelachvili, J. *J. Colloid Interface Sci.* **1994**, *165*, 367.
(18) Senden, T. J.; Drummond, C. J. *Colloids Surf.* **1995**, *94*, 29.
(19) Leckband, D. E.; Helm, C. A.; Israelachvili, J. *Biochemistry* **1993**, *32*, 1127.
(20) Mozhaev, V. V.; Berezin, I. V.; Martinek, K. *Crit. Rev. Biochem.* **1988**, *3*, 235.
(21) Mozhaev, V. V.; Siksnis, V. A.; Melik-Nubarov, N. S.; Galkantaite, N. Z.; Denis, G. J.; Butkus, E. P.; Zaslavsky, B. Y.; Mestechkina, M.; Martinek, K. *Eur. J. Biochem.* **1988**, *173*, 147.
(22) Perutz, M. F. *Science* **1978**, *201*, 1187.

10.1021/la0006059 CCC: $20.00
Published on Web 12/20/2000

Understanding of these phenomena requires the study of interactions between heterogeneous surfaces that consist of hydrophobic and hydrophilic areas. Without such an understanding the structural and dynamical properties of macromolecules in aqueous solutions as well as forces between different surfaces cannot be accurately characterized and predicted.

In this paper we initiate a systematic study of interactions between heterogeneous surfaces. The effect of surface heterogeneity on intermolecular interactions between surfaces is investigated. We demonstrate that indeed hydrophobic and hydrophilic interactions are not additive and that the net interaction between patchy surfaces depends on the relative size of hydrophobic and hydrophilic sites on the surface. The surfaces studied consist of stripes of polar and nonpolar self-assembled monolayers (SAMs) of 16-alkanethiols. Measurements were performed between a 20 μm hydrophobic sphere and patterned SAMs.

Since both thiols had 16 C atoms, the topography of the patterned surface is relatively undifferentiated. Thus, the height mode imaging, obtained with the atomic force microscope (AFM), gives us no information on the distribution of the two different thiols. Lateral force microscopy (LFM), on the other hand, identifies and maps relative differences in surface frictional characteristics, allowing us to identify the surface compositional differences. Our results are an application of chemical force microscopy (CFM) where the tip is functionalized with one chemical species and scanned over the sample to detect adhesion differences between the species on the tip and those on the surface of the sample.[26] A novel mode of data acquisition was also employed, which combines the AFM's capabilities to accurately measure forces and to position the tip with nanometer precision on the surface: force mapping.[27] Force maps are arrays of force curves or force plots recorded as the tip raster-scans the sample surface and enable us to correlate specific tip−sample interactions with specific features on the sample surface. Force curves have been analyzed in different ways to get information about adhesion forces and jump into contact distances.

Materials and Methods

Standard 100 μm V-shaped silicon nitride AFM cantilevers with pyramidal tips (Digital Instruments, Santa Barbara, CA) were used for the LFM, CFM, and force mapping measurements. The colloid probe tips were prepared as follows. A glass sphere (SPI Supplies, West Chester, PA) of radius approximately 10 μm (the radius was measured by optical microscopy) was attached to the cantilever with an epoxy resin, Epon Resin 1004F (Shell Chemical, Houston, TX). A heated thin copper wire (~30 μm diameter) attached to a three-dimensional translation stage was used to position a small portion of the glue near the apex of the cantilever. Another clean wire was used to put a glass sphere onto the tip. The cantilever was heated just enough to melt the Epon and secure the particles in place.

Substrates of the desired size were cut from Si(100) wafers (WaferNet, San Jose, CA; test grade). These substrates and colloid probe tips were coated by thermal evaporation with 250−500 Å of gold (99.999%; Alfa, Ward Hill, MA). Care was taken to avoid overheating the colloid probe tips or evaporating too much gold on them since in both cases the cantilevers bend. The spring constant of the gold-coated colloid probe tips was determined using the resonant frequency method.[28] An average value of 2.98 N/m was used in this study after calibrating 20 colloid probe tips from our wafer. An increase in cantilever stiffness results in a decrease in sensitivity of the force measurement, but it enables the measurement of pull-off forces in strongly adhesive systems.

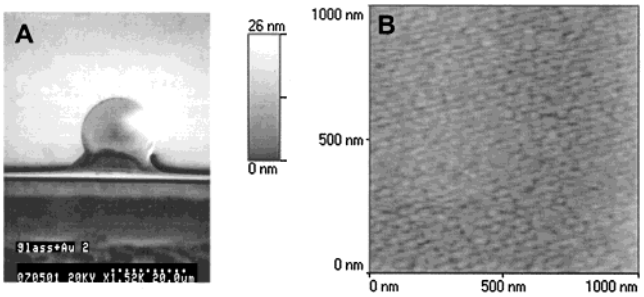

Figure 1. (A) SEM picture of a gold-coated glass sphere, 20 μm in diameter, attached to the AFM cantilever. (B) AFM image of a gold-coated glass surface acquired in water with a regular silicon nitride tip. A low pass filter was applied on the image.

Hydrophobic spheres were prepared by forming SAMs of hexadecanethiol (Aldrich, Milwaukee, WI) on the gold-coated probes.[29−31] The 16-mercaptohexadecanoic acid was synthesized in our laboratory according to the protocol of Bain et al.[29] For convenience, we will refer to a specific monolayer film according to the tail group or its wetting behavior. A hexadecanethiol film thus will be called a methyl surface or a hydrophobic surface, while the film derived from the 16-mercaptohexadecanoic acid will be referred to as the acid surface or a hydrophilic surface. Patterned SAMs with hydrophobic and hydrophilic regions on a gold surface, with dimensions of 0.2−3 μm, were formed by the microcontact printing technique.[32−35]

Surface force measurements were performed using a commercial AFM, a Nanoscope E (Digital Instruments, Santa Barbara, CA). All experiments were carried out at room temperature. To minimize the drift effects we warmed the AFM for at least 0.5 h before an experiment. The piezo drift in our experimental system was measured to be 2.5−8.5 nm/min. The time to acquire a force map is about 5 min, so at the end of the scan the drift is less than 45 nm. The delay time from one measurement to another varied. Force data were converted to force−distance curves using the method developed by Ducker et al.[14,36]

Results and Discussion

Figure 1A shows an SEM picture of a gold-coated glass sphere attached to the AFM cantilever, and Figure 1B shows an AFM image of a gold-coated glass surface. For all surfaces examined the gold coating was homogeneous. SAM surfaces were first characterized by using a silicon nitride tip to image the substrate surface. For all systems, the substrate was smooth, showing regions (15 μm × 15 μm) where the root-mean-square roughness was less than half a nanometer. Figure 2A,B gives the topography and LFM image of a patterned SAM surface, respectively. The topography image shows no contrast between the methyl and acid surfaces. However topographic images give

(23) Aizenberg, J.; Black, A. J.; Whitesides, G. M. *Nature* **1999**, *398*, 495.
(24) Delamarche, E.; Bernard, A.; Schmid, H.; Michel, B.; Biebuyck, H. *Science* **1997**, *276*, 779.
(25) Chen, C. S.; Mrksich, M.; Huang, S.; Whitesides, G. M.; Ingber, D. E. *Science* **1997**, *276*, 1425.
(26) Frisbie, C. D.; Rozsnyai, L. F.; Noy, A.; Wrighton, M. S.; Lieber, C. M. *Science* **1994**, *265*, 2071.
(27) Radmacher, M.; Cleveland, J. P.; Fritz, M.; Hansma, H. G.; Hansma, P. K. *Biophys. J.* **1994**, *66*, 2159.
(28) Cleveland, J. P.; Manne, S.; Bocek, D.; Hansma, P. K. *Rev. Sci. Instrum.* **1993**, *64* (2), 403.
(29) Bain, C. D.; Troughton, E. B.; Tao, Y.-T.; Evall, J.; Whitesides, G. M.; Nuzzo, R. G. *J. Am. Chem. Soc.* **1989**, *111*, 321.
(30) Nuzzo, R. G.; Dubois, L. H.; Allara, D. L. *J. Am. Chem. Soc.* **1990**, *112*, 558.
(31) Pan, W.; Durning, C. J.; Turro, N. J. *Langmuir* **1996**, *12*, 4469.
(32) Kumar, A.; Whitesides, G. M. *Appl. Phys. Lett.* **1993**, *63*, 2002.
(33) Kumar, A.; Biebuyck, H. A.; Whitesides, G. M. *Langmuir* **1994**, *10*, 1498.
(34) Biebuyck, H. A.; Whitesides, G. M. *Langmuir* **1994**, *10*, 2790.
(35) Larsen, N. B.; Biebuyck, H.; Delamarche, E.; Michel, B. *J. Am. Chem. Soc.* **1997**, *119*, 3017.
(36) Ducker, W. A.; Senden, T. J.; Pashley, R. M. *Nature* **1991**, *353*, 239.

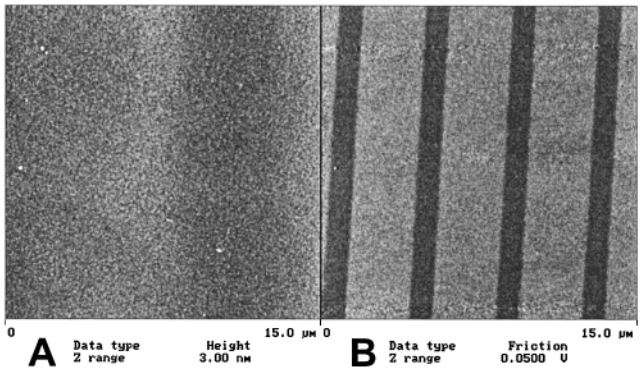

Figure 2. AFM images of a patterned SAM composed of 3 μm wide hydrophilic stripes and 1 μm wide hydrophobic stripes. The images were acquired simultaneously with a regular silicon nitride tip in air. A low pass filter was applied on both images. (A) Topography of the $-$COOH/$-CH_3$ patterned gold substrate. The root-mean-square roughness of this area is 0.281 nm. (B) LFM image of the surface. Areas exhibiting high lateral forces appear bright, and areas exhibiting low lateral forces appear dark.

information about surface roughness. The root-mean-square roughness of the surface shown in Figure 2 is 0.281 nm. On the other hand, LFM detects changes in the chemical functionality in adjacent regions of patterned SAMs terminated by $-CH_3$ or $-$COOH, showing the location of the hydrophobic and hydrophilic areas. This effect has been observed in several studies.[37−39]

In this paper we study the interactions between a 20 μm hydrophobic sphere and a heterogeneous surface, which consists of hydrophobic and hydrophilic stripes of controlled width, as they approach and as they are pulled apart. To understand the different forces involved in this system we first examined interactions between homogeneous surfaces. Primarily, the interactions of a hydrophobic substrate and sphere across aqueous electrolytes were investigated.[40] Different ion types (NaCl, Na_2SO_4, and $CaCl_2$) were used at concentrations of $10^{-4}-1$ M. No repulsive forces were measured, at all salt concentrations, suggesting that ions do not bind specifically to the methyl terminated thiols. Jump-in distances were larger than could be expected for pure van der Waals interactions. In addition, the pull-off forces increased as the ion concentration was increased. These observations are significant to this study, as we are able to enhance contrast between hydrophobic and hydrophilic regions by changing electrolyte concentration.

The second pair of surfaces investigated was a 20 μm hydrophobic sphere and a hydrophilic substrate, where the strength of the adhesive force was found to increase with NaCl concentration.[41] On approach, the interactions of the charged and uncharged surfaces were repulsive, with the repulsive interaction being screened as the ion concentration is increased. The repulsions between $-CH_3$ and $-$COOH surfaces were due to the compression of the double layer of the charged surface ($-$COOH) by the presence of the uncharged ($-CH_3$) sphere and were accurately described as corresponding to two surfaces of different charge interacting with surface charges that are independent of separation (i.e., the constant charge model). In a previous work we have demonstrated that the charge on the carboxylic acid terminated thiol surface can be understood if the acid groups have a pK_a of 6.3 and sodium ions bind with a binding constant of p$K_{Na} = 3.7$.[41,42] This competitive site binding model demonstrates that the acid surface charge is around 5% of the maximum possible.

As mentioned in the Introduction, our system is a hydrophobic sphere and a heterogeneous surface. The degree of surface heterogeneity is characterized by the parameter λ, where λ is the ratio of the width of the hydrophilic stripe to the width of the hydrophobic stripe and it ranges from 0.5 to 7.2. Of significance to this study is also the ratio of the particle radius to the stripe size. For our studies the particle had a radius of 10 μm and this ratio ranged from 3.5 to 37. From the above it is clear that if the ratio of the particle radius to the stripe width becomes very small (smaller than 0.5), either by using a very sharp tip or by producing very large stripes compared to the particle radius, then the heterogeneous patterning will not affect the overall force that the sphere experiences. Furthermore, we are interested in the interaction of the sphere with a surface at small separations. Typical separations of interest are 1−40 nm (0.1−3 Debye lengths for a concentration of 5×10^{-4} M NaCl). Thus we are working in the small stripe, small separation limit. In addition, we work at ionic strengths where the characteristic length of the electrostatic repulsion, $1/\kappa$ (the Debye length), is 1.36−13.6 nm. The jump-in distances which can be used to characterize the length scale of hydrophobic−hydrophilic interactions is a measure of the particle−surface separation where the slope of the force distance curve equals the spring constant of the cantilever. This distance thus depends on the particle size, the cantilever, and the details of the attractive forces. Nevertheless, this jump-in distance characterizes the distance over which the attractive forces are of significance. This distance increases with salt concentration and lies in the range of 1.5−15 nm for different heterogeneous surfaces. The "effective interaction area" between a sphere and a flat surface is given by the Langbein approximation:[43]

$$A_{\text{eff}} = 2\pi RD \qquad (1)$$

Here R is the radius of the sphere and D is the surface separation distance. For $R = 10$ μm and $D = 10$ nm, eq 1 gives $A_{\text{eff}} = 6.3 \times 10^{-13}$ m^2, which corresponds to an area of radius 450 nm. Thus, the particle will sample only one to two stripes as it is brought closer to the surface.

The force mapping technique was used to measure forces between the heterogeneous surfaces and the sphere. As explained in the Introduction, an area is selected and forces are measured (both approach and retraction) as the sphere rasters the patterned surface. The 32 × 32 forces are measured for the selected area and are analyzed to determine jump-in distances and pull-off forces. Adhesion data, for each one of the 32 × 32 forces, are then represented by a pixel. High adhesion data are shown with a dark pixel, whereas low adhesion is shown with a light color.

The first heterogeneous surface that we studied is a patterned SAM that consists of 1.4 μm wide hydrophilic stripes and 2.9 μm wide hydrophobic stripes, $\lambda = 0.48$. On approach, the hydrophobic sphere feels only repulsions independent of the location of the sphere relative to the

(37) Wilbur, J. L.; Biebuyck, H. A.; MacDonald, J. C.; Whitesides, G. M. *Langmuir* **1995**, *11*, 825.
(38) van der Vegte, E. W.; Hadziioannou, G. *Langmuir* **1997**, *13*, 4357.
(39) Zhou, Y.; Fan, H.; Fong, T.; Lopez, G. P. *Langmuir* **1998**, *14*, 660.
(40) Kokkoli, E.; Zukoski, C. F. *Langmuir* **1998**, *14*, 1189.
(41) Kokkoli, E.; Zukoski, C. F. *J. Colloid Interface Sci.* **2000**, *230*, 176.
(42) Kokkoli E.; Zukoski, C. F. *Langmuir* **2000**, *16*, 6029.
(43) Israelachvili, J. *Intermolecular & Surface Forces*; Academic Press: New York, 1992.

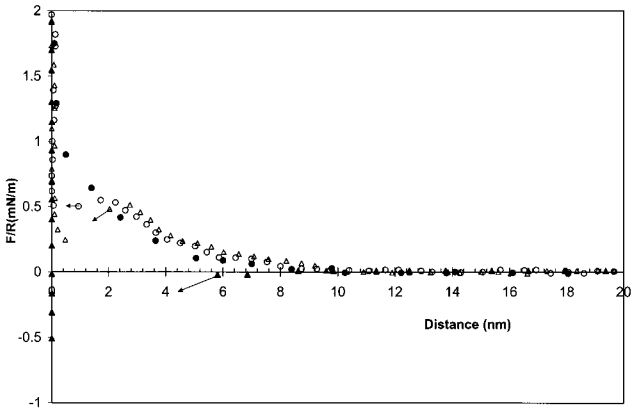

Figure 3. Normalized forces in 0.01 M NaCl scaled by the radius of the sphere. The arrows indicate the jump-in distances. Three different hydrophobic spheres were used. Filled symbols correspond to measurements between two homogeneous surfaces, and two different spheres and open symbols correspond to measurements between two different areas of a heterogeneous surface and the same hydrophobic sphere. The patterned surface consists of 1.4 μm wide hydrophilic stripes and 2.9 μm wide hydrophobic stripes. Key: (▲) force between a 20 μm hydrophobic sphere and a homogeneous hydrophobic surface; (●) force between a 20 μm hydrophobic sphere and a homogeneous hydrophilic surface; (△) force between a 20 μm hydrophobic sphere and a hydrophobic site of the heterogeneous surface; (○) force between a 20 μm hydrophobic sphere and a hydrophilic site of the heterogeneous surface.

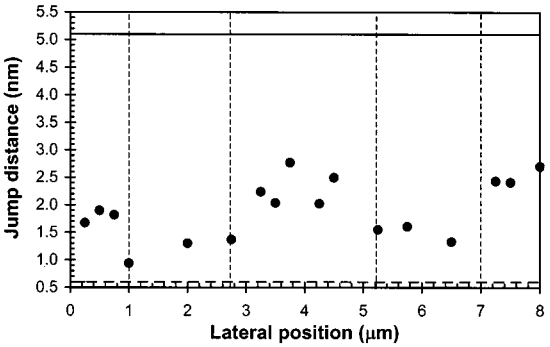

Figure 4. Jump-in distances versus the lateral position across a patterned SAM that consists of 1.4 μm wide hydrophilic stripes and 2.9 μm wide hydrophobic stripes. The vertical dashed lines indicate where the different zones are. Jump into contact distances were measured between the patterned surface and a 20 μm hydrophobic sphere in 0.01 M NaCl. For comparison, jump-in distances are shown for the case of two pure hydrophobic SAMs (solid line) and one hydrophobic sphere interacting with a hydrophilic SAM (dashed line) across 0.01 M NaCl.

one on the surface. In water and small concentrations of NaCl, and independent of whether the hydrophobic sphere is positioned on top of a hydrophobic or hydrophilic area, the repulsions have similar strengths and decay lengths. Only when the surfaces are separated by couple of nanometers apart can the hydrophobic sphere distinguish between the hydrophobic and hydrophilic areas. Figure 3 shows force versus separation profiles between a hydrophobic sphere and two different sites of the heterogeneous surface, one hydrophobic and one hydrophilic, at 0.01 M NaCl. For comparison we have also included force curves between homogeneous systems. The $-CH_3/-CH_3$ interaction on the heterogeneous surface is repulsive with a jump into contact at 2 nm whereas the interaction between two homogeneous hydrophobic surfaces is purely attractive with a jump into contact at 5.8 nm. On approach the interaction of a hydrophobic sphere with a homogeneous hydrophilic surface is repulsive while the $-CH_3/-$COOH interaction on the heterogeneous surface was more repulsive up to about 1 nm where the surfaces jumped into an adhesive contact. Figure 4 shows jump-in distances as a function of lateral position on the heterogeneous surface. To generate these data, force curves have been analyzed along one line with a spacing of 250 nm between individual force curves. Depending on whether the sphere is positioned on top of a hydrophobic or a hydrophilic site, the two surfaces will jump into contact at a different separation. Results are shown for 0.01 M NaCl. When the hydrophobic sphere is on top of a hydrophobic area, the sphere will jump into contact from a distance of approximately 2.23 nm, and when it is positioned on top of a hydrophilic area, the jump-in distance will be around 1.35 nm. For two pure methyl SAM surfaces in 0.01 M NaCl, jump-in distances are around 5−6 nm,[40] while, for a homogeneous acid and methyl SAM interaction, the jump-in distance is less than 1 nm.[41] Direct comparisons between different interactions are difficult to make as different spheres were used in each experiment (unless stated otherwise). Previous work has shown that surface asperities on the spheres can produce quantitatively different force curves.[40] Nevertheless, qualitative comparisons remain valid. However, even given these uncertainties, our previous studies indicate that the differences observed here are outside the measurement uncertainties. These differences are reproducible and indicate subtle but significant changes in the interaction forces.

The results shown in Figures 3 and 4 suggest that when dealing with heterogeneous hydrophobic and hydrophilic surfaces predictions cannot be made on the basis of measurements made on homogeneous surfaces and that, to a certain degree, the hydrophobic interactions are neutralized in the presence of hydrophilic interactions. If hydrophobic and hydrophilic interactions were additive, we would expect to measure repulsions only when the sphere is on top of the hydrophilic areas of the substrate and attractions when the sphere is on top of the hydrophobic areas. We would also expect the jump-in distances to be in the order of 5−6 nm for the $-CH_3/-CH_3$ interactions and less than 1 nm for the $-CH_3/-$COOH interaction. Instead, our results indicate that perhaps the hydrophobic interaction has been neutralized. The ratio of the hydrophobic sphere to the width of the hydrophilic stripes is large (20:1.5). As a result, we might expect some averaging effect of the interactions to take place, with the hydrophobic interactions to dominate. The key observation is that the repulsive rather than the attractive forces dominate.

Figure 5 shows the variation of jump-in distances with position on the surface for $\lambda = 0.9$, in 5×10^{-4} M NaCl. Force curves have been recorded while scanning along one line with a spacing of 125 nm between individual force curves. For this system, there is no difference on the jump-in distances between the hydrophobic sphere and the hydrophobic and hydrophilic portions of the patterned surface. These results indicate that as the hydrophobic sphere is approaching the heterogeneous surface with $\lambda = 0.9$, the force profile will be exactly the same if the sphere contacts the methyl or acid portions of the patterned surface (i.e., repulsion decays with the same decay length and the jump into contact distances will be the same), independent of lateral position. Comparisons of Figures 4 and 5 reveal that when $\lambda \approx 1$ jump-in distances are abnormally high at 10−17.3 nm, which is about 2−4 times higher than the jump-in distances observed between two pure hydrophobic SAMs. We emphasize that the large jump-in distances observed for $\lambda \approx 1$ are reproducible and

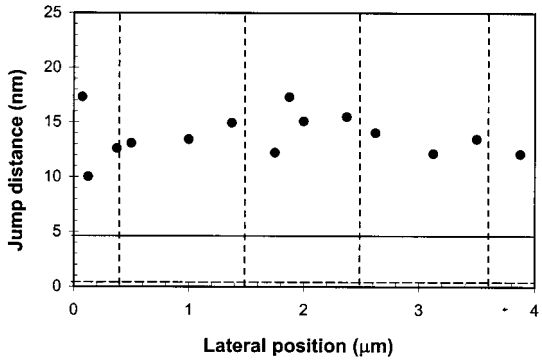

Figure 5. Jump-in distances versus the lateral position across a patterned SAM that consists of 0.95 μm wide hydrophilic stripes and 1.05 μm wide hydrophobic stripes. The vertical dashed lines indicate where the different zones are. Jump into contact distances were measured between the patterned surface and a 20 μm hydrophobic sphere in 5×10^{-4} M NaCl. For comparison, jump-in distances are shown for the case of two pure hydrophobic SAMs (solid line) and one hydrophobic sphere interacting with a hydrophilic SAM (dashed line) in 5×10^{-4} M NaCl.

extensive care was taken to ensure that surfaces are not contaminated.

We conclude that when $\lambda \neq 1$, the jump-in distance is sensitive to the surface onto which the sphere jumps into contact. However, when there is an equal amount of hydrophobic and hydrophilic sites on the surface, we observe no contrast in surface properties (i.e., the different surface interactions have averaged). Thus, when the 20 μm hydrophobic sphere approaches a surface where $\lambda \approx 1$ (with stripes of 1−2 μm), the sphere is unable to distinguish the stripe type up to and including the distance where the gradient of the force matches the cantilever constant and the probe jumps into contact. In addition, our results demonstrate that the attraction between a hydrophobic sphere and a patterned SAM with $\lambda \approx 1$ is long range and exceeds that observed for hydrophobic SAMs under nearly identical conditions.

Force mapping was used to study the strength of adhesion between the hydrophobic sphere and different heterogeneous surfaces in water and different concentrations of NaCl. Force volume (FV) images, based on adhesion data, were constructed from 1024 force plots on the sample surface (32 force plots per line × 32 lines). Force curves have been analyzed and the adhesion (pull-off force) is determined. A two-dimensional map of the pull-off force is constructed with high adhesion represented as a dark color pixel and low adhesion shown with a light color pixel. The FV images that we show here are therefore two-dimensional arrays of adhesion data as a function of lateral position on the patterned surface.

Figure 6B−E shows FV images for a heterogeneous surface with 1.4 μm wide hydrophilic stripes and 2.9 μm wide hydrophobic stripes ($\lambda = 0.48$), in water and different concentrations of NaCl. The CFM image of the heterogeneous surface, taken with the hydrophobic sphere, is shown in Figure 6A. Comparison of Figure 6A with Figure 6B reveals that FV images, based on adhesion data, provide useful information about the chemistry of the surface. FV images differentiate between areas of high and low adhesion the same way that CFM identifies and maps relative differences in surface frictional characteristics. Both FV and CFM images are therefore useful tools in identifying surface compositional differences that are otherwise unrevealed by height imaging. This observation indicates that there is a connection between adhesion and friction. As the electrolyte concentration is increased the

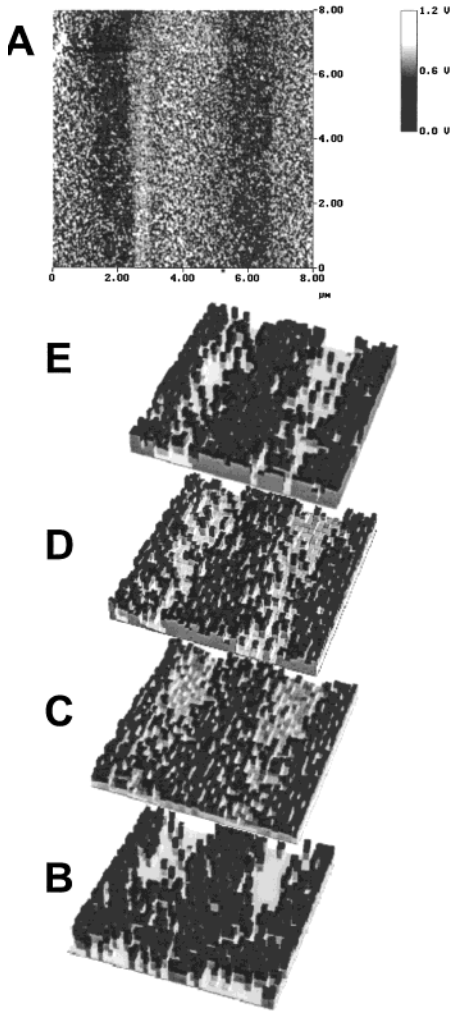

Figure 6. (A) CFM image of a patterned SAM that consists of 1.4 μm wide hydrophilic stripes and 2.9 μm wide hydrophobic stripes acquired with a 20 μm hydrophobic sphere in 5×10^{-4} M NaCl. A low pass filter was applied on the image. Areas exhibiting high lateral forces appear bright and areas exhibiting low lateral forces appear dark. (B) FV image for the surface shown in (A) and the 20 μm hydrophobic sphere, in water. (C) FV image in 5×10^{-3} M NaCl. (D) FV image in 0.01 M NaCl. (E) FV image in 0.03 M NaCl. In the FV images, high adhesion data are represented with a dark pixel and low adhesion areas are shown with a light color pixel.

contrast between the high and low adhesion areas (i.e., between the methyl and acid areas) grows.

The effect of electrolyte on FV images for a heterogeneous surface that consists of 0.95 μm wide hydrophilic stripes and 1.05 μm wide hydrophobic stripes is shown in Figure 7B−E. The CFM image that was acquired with a 20 μm hydrophobic sphere showed no contrast. An LFM image of the surface is given in Figure 7A, taken with a regular silicon nitride tip. For this surface, $\lambda = 0.9$, and a 20 μm hydrophobic sphere, FV images revealed that the contrast between high and low adhesion areas (i.e., between $-CH_3$ and $-COOH$ areas) is minimal. Since the CFM image that was acquired with the 20 μm hydrophobic sphere showed no contrast as well, this is another indication that there is a clear connection between adhesion and friction. For example, in water (Figure 7B) the FV image does not reconstruct the surface shown in Figure 7A. When the salt concentration is increased to 0.03 M NaCl (Figure 7E), hydrophobic patches on the surface are evident. However, stripe orientation is far from clear. Thus, when the surface is composed of hydrophobic

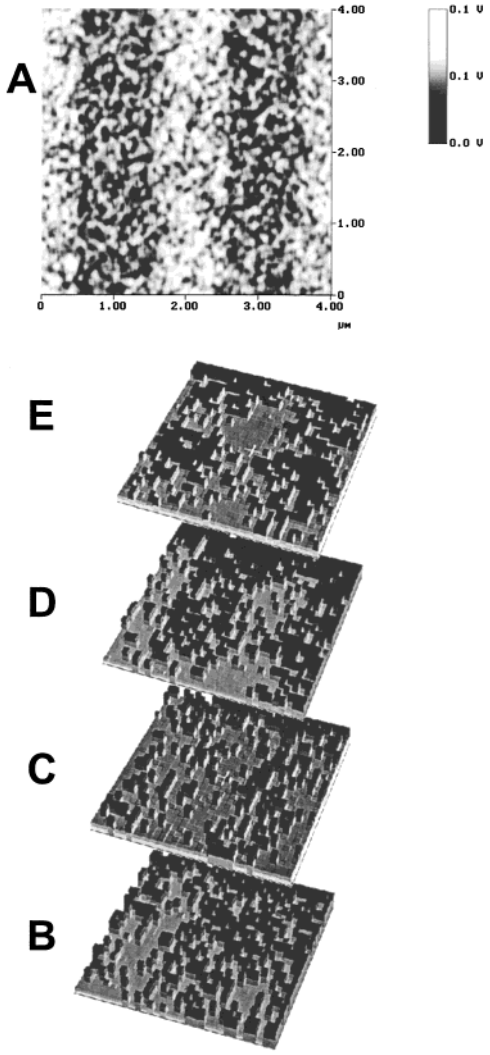

Figure 7. (A) LFM image of a patterned SAM that consists of 0.95 μm wide hydrophilic stripes and 1.05 μm wide hydrophobic stripes acquired with a regular silicon nitride tip in air. A low pass filter was applied on the image. Areas exhibiting high lateral forces appear bright, and areas exhibiting low lateral forces appear dark. (B) FV image for the surface shown in (A) and the 20 μm hydrophobic sphere, in water. (C) FV image in 5×10^{-3} M NaCl. (D) FV image in 0.01 M NaCl. (E) FV image in 0.03 M NaCl. In the FV images, high adhesion data are represented with a dark pixel and low adhesion areas are shown with a light color pixel.

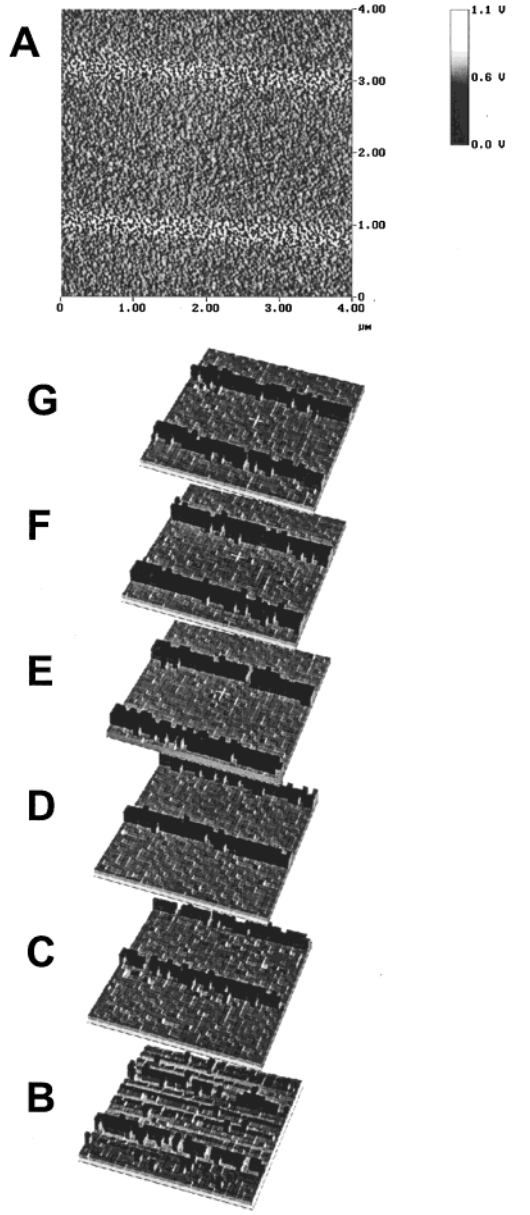

Figure 8. (A) CFM image of a patterned SAM that consists of 1.97 μm wide hydrophilic stripes and 0.27 μm wide hydrophobic stripes acquired with a 20 μm hydrophobic sphere in 0.05 M NaCl. A low pass filter was applied on the image. Areas exhibiting high lateral forces appear bright and areas exhibiting low lateral forces appear dark. (B) FV image for the surface shown in (A) and the 20 μm hydrophobic sphere, in water. (C) FV image in 5×10^{-4} M NaCl. (D) FV image in 5×10^{-3} M NaCl. (E) FV image in 0.01 M NaCl. (F) FV image in 0.03 M NaCl. (G) FV image in 0.05 M NaCl. In the FV images, high adhesion data are represented with a dark pixel and low adhesion areas are shown with a light color pixel.

and hydrophilic stripes of equal size, both adhesion forces and approach curves, as discussed earlier, average over the surface giving rise to surface that behaves as if it was homogeneous.

So far we have showed results for heterogeneous surfaces with $\lambda = 0.5$ and 0.9. Figure 8 shows FV images for a patterned surface with $\lambda = 7.2$ (1.97 μm wide hydrophilic stripes and 0.27 μm wide hydrophobic stripes). In this extreme case, where the surface could easily be considered as a homogeneous hydrophilic one, the contrast between high and low adhesion sites is excellent in all conditions tried. Even though the hydrophobic stripes are only 270 nm wide, they can easily be differentiated by a 20 μm hydrophobic sphere with a contact radius of 130 nm.

The contact radius of the sphere was determined by the theory of adhesion of elastic spheres by Johnson, Kendal, and Roberts.[44] The JKR theory predicts that, under zero external load where a sphere comes into contact with a flat surface, it deforms into a flat region giving a contact circular area of radius α_o:[43]

$$\alpha_o = (12\pi R^2 \gamma_{SL}/K)^{1/3} \quad (2)$$

Here R is the radius of the sphere, γ_{SL} is the interfacial tension of the surface in liquid, and K is the elastic moduli

(44) Johnson, K. L.; Kendall, K.; Roberts, A. D. *Proc. R. Soc. London, Ser. A* **1971**, *324*, 301.

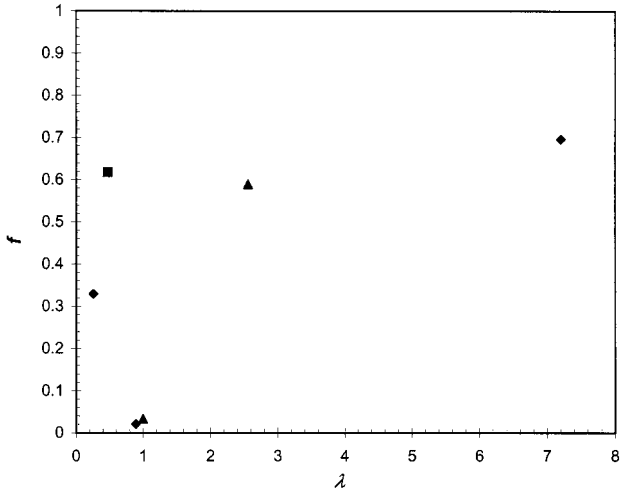

Figure 9. Adhesion data between a 20 μm hydrophobic sphere and different heterogeneous surfaces, with various λ parameters, in 5×10^{-4} M NaCl. Measurements were done with three different $-CH_3$ spheres: A (■); B (▲); C (◆). For each surface, 32 force curves were taken along one line while the sphere was scanned across the patterned surface. These forces were then analyzed, and the adhesion was calculated for each one of them. The *y* axis is the adhesion force for the hydrophobic portion of the heterogeneous surface minus the adhesion for the hydrophilic, over their sum.

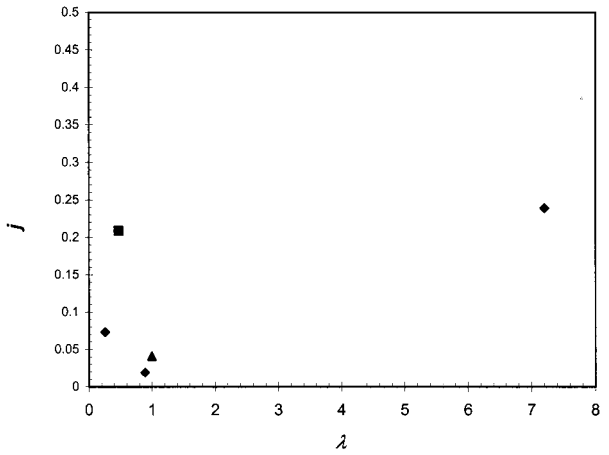

Figure 10. Jump into contact data between a 20 μm hydrophobic sphere and different heterogeneous surfaces, with various λ parameters, in 5×10^{-4} M NaCl. Measurements were done with three different $-CH_3$ spheres: A (■); B (▲); C (◆). For each surface, 32 force curves were taken along one line while the sphere was scanned across the patterned surface. These forces were then analyzed, and the jump-in distances were calculated for each one of them. The *y* axis is the jump-in distance for the hydrophobic portion of the heterogeneous surface minus the jump-in for the hydrophilic, over their sum.

of the sphere. For $R = 10$ μm, $\gamma_{SL} = 41.48$ mN/m,[45] and $K = 71.7 \times 10^9$ N/m^2,[46] eq 2 gives $\alpha_o = 130$ nm.

Note that the same sphere used to acquire FV images of the $\lambda = 7.2$ surface was used for the $\lambda = 0.9$ surface. While contrast was observed for $\lambda = 7.2$, no contrast was observed for $\lambda = 0.9$. This excludes the possibility that the high contrast seen in the $\lambda = 7.2$ case was due to a sharp asperity on the surface of the sphere.

Our results indicate that interactions between a 20 μm methyl sphere and a heterogeneous surface that has equal methyl and acid areas will average, whereas, for other values of λ, the hydrophobic sphere will clearly differentiate between the different areas (up to $\lambda \approx 7$), accurately mapping high and low adhesion areas on the surface. To demonstrate this even further, force mapping was used to measure interactions between a hydrophobic sphere and heterogeneous surfaces with various values of λ, in 5×10^{-4} M NaCl. Results are shown in Figures 9 and 10 for adhesion and jump-in distances, respectively. The parameter *f* in Figure 9 is the adhesion force for the hydrophobic portion of the heterogeneous surface minus the adhesion for the hydrophilic, over their sum, and is a measure of the adhesion contrast. The parameter *j* in Figure 10 is the jump-in distance for the hydrophobic portion of the heterogeneous surface minus the jump into contact distance for the hydrophilic, over their sum, and is a measure of the contrast in jump-in distances. When these two parameters are zero, the adhesion data and jump into contact distances are the same for both the hydrophobic and hydrophilic areas of the surface, and for any other value, different areas on the surface interact with the hydrophobic sphere in different ways. Figures 9 and 10 show that when λ is close to one, both *f* and *j* are zero. As shown in these figures, two different surfaces were used when $\lambda \approx 1$. One had 0.95 μm wide hydrophilic stripes and 1.05 μm wide hydrophobic stripes and the other one had 2.38 μm wide hydrophilic stripes and 2.38 μm wide hydrophobic stripes. No attempt was made to fabricate a heterogeneous surface for which λ would be one but would have wider stripes, as we were limited by the mask available for the photolithography. On the basis of the experiments with standard hydrophobic and hydrophilic AFM cantilevers, it is clear that the effect seen here will depend on both the size of the sphere and the width of the stripes that produce the heterogeneous surface. For example, if a sharp tip is used, instead of a 20 μm sphere, we do not see this averaging effect. Likewise, if the stripes are 100 μm wide, then interactions between this kind of surface and a 20 μm sphere are not expected to average.

At this time the origin of the averaging effect when $\lambda \approx 1$ is not clear. We speculate that the water structure next to the hydrophobic and hydrophilic surfaces may be a key parameter on this phenomenon. A hydrophilic surface will break the water structure, whereas a hydrophobic surface will enhance the water structure.[47−50] However, these effects are not additive and there has been little systematic investigation of the effect of the heterogeneities on surface forces. For the sphere and the stripe sizes studied here, approach and adhesion forces average over a heterogeneous surface when the ratio of hydrophilic to hydrophobic sites equals one. Clearly, understanding this phenomenon requires further experiments and modeling.

Conclusions

Here we demonstrate that as a 20 μm hydrophobic sphere approaches a heterogeneous surface, repulsions are measured all over the patterned surface, in water and at low NaCl concentrations. The repulsions measured between the patterned surfaces and the methyl sphere are due to the compression of the double layer next to the

(45) Kokkoli, E.; Zukoski, C. F. *J. Colloid Interface Sci.* **1999**, *209*, 60.
(46) *Handbook of Chemistry and Physics*; CRC Press: Cleveland, OH, 1975.
(47) Nickolov, Z. S.; Earnshaw, J. C.; McGarvey, J. J. *Colloids Surf.* **1993**, *76*, 41.
(48) Yalamanchili, M. R.; Atia, A. A.; Miller, J. D. *Langmuir* **1996**, *12*, 4176.
(49) Head-Gordon, T.; Sorenson, J. M.; Pertsemlidis, A.; Glaeser, R. M. *Biophys. J* **1997**, *73*, 2106.
(50) Ide, M.; Maeda, Y.; Kitano, H. *J. Phys. Chem.* **1997**, *101*, 7022.

acid patches on the surface. Independent of whether the hydrophobic sphere is positioned on top of a hydrophobic or hydrophilic area repulsions with the same strength and decay length are measured. Only when surfaces come to a separation of 2−5 nm is the hydrophobic sphere able to distinguish between the hydrophobic and hydrophilic areas, for heterogeneous surfaces of $\lambda \neq 1$. When there is an equal amount of methyl and acid sites on the surface, there is no difference between the jump-in distances measured between the $-CH_3$ sphere and the $-CH_3$ or $-COOH$ portion of the patterned surface. Under these conditions jump-in distances are abnormally high and exceed that observed for pure hydrophobic surfaces under nearly identical conditions. This result suggests that hydrophobic and hydrophilic interactions are not additive and that perhaps the hydrophobic interaction can be overwhelmed for separation distances greater than couple of nanometers.

FV images, based on adhesion data, provide useful information about the chemistry of the surface and can differentiate between areas of high and low adhesion the same way that CFM can identify and map relative differences in surface frictional characteristics. Both FV and CFM images are therefore useful tools in identifying surface compositional differences that are otherwise undetectable by height imaging. As the electrolyte concentration is increased the contrast between the high and low adhesion areas (i.e., between the hydrophobic and hydrophilic areas) is increased.

Of significance to this study is the ratio of the particle radius to the stripe size. This ratio varied from 3.5 to 37, as a heterogeneous patterning on a length scale much larger than the sphere cannot affect the force. For a heterogeneous surface, where the ratio of hydrophilic to hydrophobic sites is close to one, FV images show that the differentiation between high and low adhesion areas and, as a consequence, between hydrophobic and hydrophilic areas is minimal. It seems therefore that when the surface has hydrophobic and hydrophilic patches of equal size, both adhesion forces and approach curves average over the surface giving rise to a surface that behaves as if it was homogeneous.

At this time the origin of the averaging effect when $\lambda \approx 1$ is not clear. We speculate that the water structure next to the hydrophobic and hydrophilic surfaces may be a key parameter on this phenomenon. However these effects are not additive and there has been little systematic investigation of the effect of the heterogeneities on surface forces. Clearly, understanding this phenomenon requires further experiments and modeling.

Acknowledgment. We thank the Beckman Imaging Technology Group and the Materials Research Laboratory for the use of their Center for Microanalysis of Materials and their Microfabrication Facility. This work was supported by NASA under Grant No. NAG8-1376.

LA0006059